Available online at www.sciencedirect.com
ScienceDirect
Journal of Organometallic Chemistry 691 (2006) 4829–4842
Journal of Organometallic Chemistry
www.elsevier.com/locate/jorganchem

Supramolecular chemistry of half-sandwich organometallic building blocks based on $RuCl_2$(*p*-cymene)Ph_2PCH_2Y

Sandra E. Dann [a], Sean E. Durran [a], Mark R.J. Elsegood [a], Martin B. Smith [a,*], Paul M. Staniland [a], Salem Talib [a], Sophie H. Dale [b]

[a] *Department of Chemistry, Loughborough University, Loughborough, Leics LE11 3TU, UK*
[b] *Molecular Profiles Ltd., 8 Orchard Place, Nottingham Business Park, Nottingham NG8 6PX, UK*

Received 26 June 2006; received in revised form 18 July 2006; accepted 18 July 2006
Available online 10 August 2006

Abstract

A new series of neutral organometallic building blocks based on piano-stool ruthenium(II) complexes, $RuCl_2$(*p*-cymene)Ph_2PCH_2Y [Y = -NHC_6H_4(2-CO_2H) (**2a**), -NHC_6H_4(3-CO_2H) (**2b**), -NHC_6H_3(3-CO_2H)(6-OCH_3) (**2c**), -NHC_6H_4(4-CO_2H) (**2d**), -NHC_6H_3(2-CO_2H)(4-OH) (**2e**), -NHC_6H_3(3-OH)(4-CO_2H) (**2f**), -NHC_6H_3(2-CO_2H)(5-CO_2H) (**2g**) and -OH (**2h**)], were synthesised in high yields (>88%) from $\{RuCl_2(p\text{-cymene})\}_2$ and the appropriate phosphines **1a**–**1h**. The new tertiary phosphine **1b** was prepared by Mannich condensation of $NH_2C_6H_4$(3-CO_2H) with Ph_2PCH_2OH in MeOH. Solution NMR ($^{31}P\{^1H\}$, ^1H), FT-IR and microanalytical data are in full agreement with the proposed structures. Single crystal X-ray studies confirm that, in each case, compounds **2a**, **2b** and **2d**–**2h** have piano-stool arrangements with typical Ru–P, Ru–Cl and Ru–$C_{centroid}$ bond lengths. From our crystallographic studies, factors that influence the supramolecular assemblies of these ruthenium(II) complexes include: (i) the type of functional group present, (ii) the geometric disposition of the –$N(H)CH_2PPh_2$, –CO_2H and –OH groups around the central benzene scaffold, and (iii) the solvents used in the recrystallisations. Hence in isomers **2a** and **2b**, molecules are associated into head-to-tail dimer pairs through classical intermolecular O–H···O hydrogen bonding. This feature is also observed in isomer **2d** but dimer pairs are further associated to give a 1-D chain through assisted intermolecular N–H···Cl hydrogen bonding. The additional 4-hydroxo group in **2e** promotes a ladder arrangement via intermolecular O–H···O and O–H···Cl hydrogen bonding. In contrast the isomeric compound **2f** does not show head-to-tail O–H···O hydrogen bonding but instead O–H···Cl and N–H···O intermolecular hydrogen bonding is observed. Depending on the choice of solvent (MeOH or DMSO), **2g** forms extended networks based on chains (**2g · DMSO · 1.5MeOH**) or tapes (**2g · 3MeOH**). In **2h**, a single intramolecular O–H···Cl hydrogen bond is observed for each independent molecule. The X-ray structure of one representative tertiary phosphine, **1f**, has also been determined.

Keywords: Phosphine ligands; Ruthenium(II); Supramolecular chemistry; Organometallic complexes; X-ray crystallography

1. Introduction

There has been considerable interest in the chemistry of M(arene) (M = Ru, Rh, Ir; arene = η^6-*p*-cymene, η^5-Cp^*, etc.) organometallic moieties for a variety of purposes. These range from their interesting and varied coordination chemistry [1–3] including DNA binding studies [4–6] to applications in areas such as chemosensors/highly selective receptors [7,8] and catalysis [9–12]. Furthermore these organometallic fragments have been used in the synthesis of cyclometallated [13–15] and chiral half-sandwich compounds [16,17]. Metal arenes have also been employed in the controlled stepwise assembly of organometallic supramolecular squares and rectangles [18,19] and, more

* Corresponding author. Tel.: +44 1509 222553; fax: +44 1509 223925.
E-mail address: m.b.smith@lboro.ac.uk (M.B. Smith).

0022-328X/$ - see front matter © 2006 Elsevier B.V. All rights reserved.
doi:10.1016/j.jorganchem.2006.07.036

recently, water-soluble heterobimetallic coordination polymers containing $CpRu^+$ (and $AgCl_2^-$) have been synthesised by Peruzzini and co-workers [20]. Prior to our work, and as far as we are aware, the supramolecular chemistry of mononuclear Ru(arene) organometallic complexes utilising hydrogen bonding interactions has not been studied [21]. Other groups have described crystal engineering studies using metal-arene organometallic components based on either Cr [22], Mn [23], Fe [24], Co [24] or Rh [25].

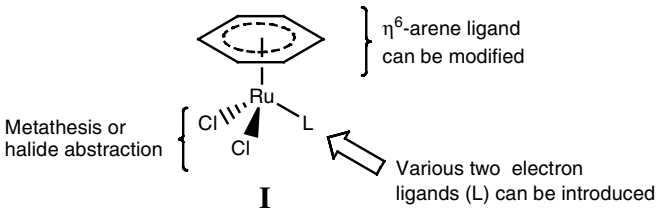

I

Our rationale to a standardised study of self-assembly and supramolecular behaviour within a series of organometallic ruthenium(II) complexes led us to analyse the key structural features of a piano-stool compound such as **I**. Inspection of **I** reveals three potential routes by which manipulation of the ligands can be used to influence hydrogen bonded supramolecular architectures. Bis sandwich compounds have been prepared via halide abstraction of the chloride ligands, using a silver(I) salt such as CF_3SO_3Ag, from $\{RuCl_2(p\text{-cymene})\}_2$ or $\{RuCl(Cp^*)\}_4$ in acetone or THF/MeCN and subsequent incorporation of other arene ligands with H-bonding capabilities [26]. Alternatively arene functionalisation with polar appendages (e.g. OH, NH_2) suitable for H-bonding have been described although their synthetic procedures are non-trival [27]. Moreover from X-ray crystallographic studies, secondary interactions tend to be restricted to intramolecular O–H···Cl [27b] or intermolecular O–H···Cl [27c] H-bonding. Neutral two-electron donor ligands such as tertiary phosphines, PR_3, are known to readily cleave Ru–Cl-Ru bridges [28] such as $\{RuCl_2(p\text{-cymene})\}_2$ to give mononuclear $RuCl_2(p\text{-cymene})(PR_3)$ complexes. Typically in these examples all three R substituents on phosphorus are equivalent and either alkyl or aryl based. We are unaware of any systematic studies exploring the supramolecular chemistry of $RuCl_2(p\text{-cymene})(PR_3)$ with phosphines from a similar ligand library. As part of ongoing studies in our group [29–35] we have used Mannich-based condensation reactions as an excellent procedure for synthesising highly functionalised tertiary and ditertiary phosphines. Herein we describe the use of isomeric, carboxylic acid or mixed phenol/carboxylic acid containing tertiary phosphines, Ph_2PCH_2Y, for the preparation of a range of $RuCl_2(p\text{-cymene})(Ph_2PCH_2Y)$ complexes. These piano-stool compounds have been characterised by spectroscopic ($^{31}P\{^1H\}$, ^1H NMR) and analytical methods. Furthermore single crystal X-ray structures have been determined for a selection of these compounds and reveal that (i) the nature of the substituent influences the solid state structures, (ii) the predisposition of functional groups around the central benzene core is crucial, and (iii) the choice of recrystallising solvent is important in controlling the hydrogen bonded supramolecular assemblies of these organometallic compounds.

2. Experimental

Standard Schlenk techniques were used for the synthesis of **1b** whilst all other reactions were carried out in air using previously distilled solvents unless otherwise stated. The ligands **1a** and **1c–1h** have been reported elsewhere [32,36] and the metal precursor $\{RuCl_2(p\text{-cymene})\}_2$ prepared according to a known procedure [37]. All other chemicals were obtained from commercial sources and used directly without further purification.

Infrared spectra were recorded as KBr pellets in the range 4000–200 cm^{-1} on a Perkin–Elmer System 2000 Fourier-transform spectrometer, ^1H NMR spectra (250 or 400 MHz) on a Bruker AC250 FT spectrometer with chemical shifts (δ) in ppm to high frequency of $Si(CH_3)_4$ and coupling constants (J) in Hz, $^{31}P\{^1H\}$ NMR spectra were recorded on JEOL FX90Q or Bruker DPX-400 FT spectrometers with chemical shifts (δ) in ppm to high frequency of 85% H_3PO_4. All NMR spectra were measured in $CDCl_3$ unless otherwise stated. Elemental analyses (Perkin–Elmer 2400 CHN Elemental Analyzer) were performed by the Loughborough University Analytical Service within the Department of Chemistry.

2.1. Preparation of *1b*

The amine $NH_2C_6H_4(3\text{-}CO_2H)$ (0.345 g, 2.52 mmol) and Ph_2PCH_2OH (0.557 g, 2.58 mmol) was dissolved in MeOH (HPLC grade, 10 mL) to give a yellow solution. The solution was stirred at room temperature for 5 h and evaporated to dryness under reduced pressure. Yield: 0.637 g. $^{31}P\{^1H\}$ NMR spectroscopy confirmed **1b** as the major phosphorus containing species.

2.2. Preparation of *2a–2h*

A typical procedure is given here for **2f**. To a CH_2Cl_2 (10 mL) solution of $\{RuCl_2(p\text{-cymene})\}_2$ (0.052 g, 0.085 mmol) was added **1f** (0.058 g, 0.17 mmol). The solution was stirred for 15 mins and the volume concentrated to ca. 2 mL under reduced pressure. Addition of diethyl ether (20 mL) gave an orange solid which was collected by suction filtration and dried in vacuo. Yield: 0.099 g, 88%. Yields for the other compounds prepared in this study are given in parentheses: **2a** (90%), **2c** (96%), **2d** (93%), **2e** (99%), **2g** (94%) and **2h** (92%). Microanalytical data: **2a**, $C_{30}H_{32}NO_2PRuCl_2$, requires: C, 56.17; H, 5.02; N, 2.18. Found: C, 56.11; H, 5.06; N, 3.35%. **2b**, $C_{30}H_{32}NO_2PRuCl_2 \cdot Et_2O \cdot H_2O$, requires: C, 55.66; H, 6.06; N, 1.91.

Table 1
Details of the X-ray data collections and refinements for compounds **1f**, **2a**, **2b · OEt$_2$ · H$_2$O**, **2d–2f**, **2g · 3MeOH**, **2g · DMSO · 1.5MeOH** and **2h**

Compound	**1f**	**2a**	**2b · OEt$_2$ · H$_2$O**	**2d**	**2e**	**2f**	**2g · 3MeOH**	**2g′DMSO · 1.5MeOH**	**2h**
Formula	$C_{20}H_{18}NO_3P$	$C_{30}H_{32}Cl_2NO_2PRu$	$C_{34}H_{44}Cl_2NO_4PRu$	$C_{30}H_{32}Cl_2NO_2PRu$	$C_{30}H_{32}Cl_2NO_3PRu$	$C_{30}H_{32}Cl_2NO_3PRu$	$C_{34}H_{44}Cl_2NO_7PRu$	$C_{34.50}H_{44}Cl_2NO_{6.50}PRu$	$C_{23}H_{27}Cl_2OPRu$
Molecular weight	351.32	641.51	733.64	641.51	657.51	657.51	781.64	811.71	522.39
Crystal dimensions	0.39 × 0.27 × 0.07	0.31 × 0.13 × 0.10	0.32 × 0.30 × 0.24	0.31 × 0.27 × 0.07	0.17 × 0.14 × 0.06	0.32 × 0.22 × 0.09	0.13 × 0.10 × 0.06	0.30 × 0.08 × 0.05	0.30 × 0.23 × 0.12
Crystal morphology and colour	Plate and colourless	Block and orange	Block and red	Plate and orange	Block and orange	Plate and orange	Block and red	Needle and orange	Block and orange
Crystal system	Triclinic	Monoclinic	Monoclinic	Monoclinic	Triclinic	Triclinic	Monoclinic	Monoclinic	Monoclinic
Space group	$P\bar{1}$	$P2_1/c$	$P2_1/n$	$P2_1/c$	$P\bar{1}$	$P\bar{1}$	$P2_1/n$	$P2_1/c$	$P2_1/c$
a (Å)	7.6267(9)	13.5846(6)	10.0428(5)	20.7870(8)	7.3541(4)	7.6332(3)	12.8635(11)	13.6073(6)	21.8690(11)
b (Å)	9.8428(12)	15.8035(7)	13.0085(6)	14.2415(6)	11.7103(6)	12.7330(6)	23.909(2)	23.6146(10)	7.4956(4)
c (Å)	11.9688(14)	13.8433(6)	25.7188(12)	20.8011(8)	17.0938(9)	14.5975(7)	13.0686(11)	22.6565(10)	27.2257(14)
α (°)	93.937(2)				101.894(2)	93.591(2)			
β (°)	97.013(2)	102.964(2)	90.368(2)	107.088(2)	91.946(2)	97.100(2)	118.077(2)	91.936(2)	97.296(2)
γ (°)	96.175(2)				100.604(2)	91.725(2)			
V (Å^3)	883.53(18)	2896.2(2)	3359.9(3)	5886.1(4)	1411.93(13)	1404.11(11)	3546.2(5)	7276.1(5)	4426.7(4)
Z	2	4	4	8	2	2	4	8	8
μ (mm^{-1})	0.174	0.809	0.711	0.796	0.834	0.839	0.685	0.725	1.034
θ Range (°)	2.59–28.76	1.98–29.06	1.58–29.00	1.76–29.02	1.81–29.15	1.60–29.05	1.70–29.11	1.72–25.00	2.25–28.04
Measured reflections	7845	25427	29239	51475	12716	12588	31307	52812	36919
Independent reflections	4090	7051	8147	14272	6571	6524	8627	12806	10115
Observed reflections ($F^2 > 2\sigma(F^2)$)	3212	5734	6315	9734	5425	5695	4755	7463	7237
R_{int}	0.0173	0.0227	0.0357	0.0443	0.0219	0.0148	0.1021	0.0724	0.0354
R $[F^2 > 2\sigma(F^2)]$[a]	0.0429	0.0278	0.0374	0.0422	0.0305	0.0277	0.0531	0.0504	0.0355
wR_2 (all data)[b]	0.1171	0.0626	0.0869	0.1112	0.0628	0.0686	0.1381	0.1444	0.0804
Largest difference map features (e Å^3)	0.648, −0.290	0.454, −0.359	1.082, −0.678	1.756, −0.759	0.615, −0.773	0.965, −0.320	0.802, −1.162	1.168, −0.839	0.901, −0.699

[a] $R = \sum\|F_o| - |F_c\|/\sum|F_o|$.
[b] $wR_2 = \{\sum[w(F_o^2 - F_c^2)^2]/\sum[w(F_o^2)^2]\}^{1/2}$.

Found: C, 54.98; H, 5.89; N, 2.07%. **2c**, $C_{31}H_{34}NO_3PRuCl_2$, requires: C, 55.44; H, 5.11; N, 2.09. Found: C, 55.06; H, 4.91; N, 1.82%. **2d**, $C_{30}H_{32}NO_2PRuCl_2 \cdot 0.5CH_2Cl_2$, requires: C, 53.55; H, 4.87; N, 2.05. Found: C, 53.94; H, 5.18; N, 1.95%. **2e**, $C_{30}H_{32}NO_3PRuCl_2$, requires: C, 54.80; H, 4.92; N, 2.13. Found: C, 54.28; H, 4.75; N, 2.25%. **2f**, $C_{30}H_{32}NO_3PRuCl_2 \cdot 0.5CH_2Cl_2$, requires: C, 52.32; H, 4.76; N, 2.00. Found: C, 52.48; H, 4.37; N, 1.32%. **2g**, $C_{31}H_{32}NO_4PRuCl_2$, requires: C, 54.31; H, 4.71; N, 2.04. Found: C, 53.44; H, 4.66; N, 1.90%. **2h**, $C_{23}H_{27}OPRuCl_2$, requires: C, 52.87; H, 5.22. Found: C, 52.62; H, 5.15%. The powder diffraction patterns for **2a** and **2f** fit with those calculated from single crystal data.

2.3. X-ray crystallography

Suitable crystals of **1f** were obtained upon slow evaporation to dryness of a $CDCl_3$ solution. The compounds **2a**, **2d** and **2h** were obtained by vapour diffusion of Et_2O into either a $CDCl_3$ or $CDCl_3$/MeOH solution over several days, respectively. Compound **2b** was obtained by evaporation of a CH_2Cl_2/Et_2O filtrate to dryness over several days. Suitable crystals of **2e** and **2f** were obtained by vapour diffusion of Et_2O into $CDCl_3$/MeOH solutions. For **2g** vapour diffusion of Et_2O into either $CDCl_3$/MeOH/DMSO or $CDCl_3$/MeOH solutions gave crystals suitable for single crystal X-ray crystallography. All measurements were made on a Bruker AXS SMART 1000 CCD area-detector diffractometer, at 150 K, using graphite-monochromated Mo Kα radiation ($\lambda = 0.71073$ Å) and narrow frame exposures (0.3°) in ω. Cell parameters were refined from the observed (ω) angles of all strong reflections in each data set. Intensities were corrected semiempirically for absorption based on symmetry-equivalent and repeated reflections. The structures were solved by direct methods and refined on F^2 values for all unique data by full-matrix least-squares. Table 1 gives further details. All non-hydrogen atoms were refined anisotropically. CH hydrogen atoms were placed in calculated positions (C–H 0.98–1.00 Å) and refined using a riding model. NH hydrogen atoms were located in a difference Fourier map and refined freely in all cases except compound **2g**, where restraints were applied to the N–H bond length. OH hydrogen atoms were placed in calculated positions and refined using a riding model in all cases except compounds **2f** and **2h**, where restraints were applied to the O–H bond length. Water hydrogen atoms in **2b** were located in a difference Fourier map and refined freely. U_{iso}(H) values were fixed at $1.2U_{eq}(N, C_{aromatic}, C_{methine}, C_{methylene})$ and $1.5U_{eq}(O, C_{methyl})$ in all cases except compound **2e**, where $U_{iso}(NH)$ values were freely refined. Compounds **2g · 3MeOH**, **2g · DMSO · 1.5MeOH** and **2h** were refined using disorder models. In **2g · 3MeOH**, two molecules of MeOH were disordered [major refined occupancy = 80.0(7)%] and OH hydrogen atoms were placed on the major component of the disorder model only. In **2g · DMSO · 1.5MeOH**, one

Table 2
Selected spectroscopic[a] and analytical data for compounds **1b** and **2a–2h**

Compound	δ(P)	δ(H)/arom.	δ(H)/CH_2[c]	δ(H)/*p*-$CH_3C_6H_4CH(CH_3)_2$[d]	δ(H)/*p*-$CH_3C_6H_4CH(CH_3)_2$[e]	$\nu_{OH/NH}$	ν_{CO}	*m/z*
1b[f]	−19.8	7.48–6.76	3.78 (3.8)					
2a	28.3	7.92–6.27	4.72 (5.6)	5.36, 5.18 (5.8)	2.52, 1.93, 0.84 (6.8)	3303	1648	
2b[g]	20.2	7.82–6.36	4.37 (1.8)	5.23, 5.14 (6.2)	2.46, 1.82, 0.85 (6.9)	3380, 3332	1684	641 (M)
2c	22.5	7.83–6.44	4.39	5.23, 5.12 (6.2)	2.46, 1.83, 0.83 (7.0)	3445	1705, 1676, 1595	601 (M–2Cl)
2d	20.9	7.81–6.08	4.43	5.25, 5.14 (6.2)	2.45, 1.82, 0.84 (7.0)	3353, 3309, 3291	1688, 1666, 1600	606 (M–Cl)
2e	26.3	7.90–6.09	4.63	5.34, 5.20 (6.0)	2.48, 1.90, 0.86 (6.8)	3340	1656, 1531	658 (M)
2f	20.4	7.80–5.57	4.34 (1.8)	5.23, 5.15 (6.1)	2.45, 1.82, 0.85 (6.9)	3378	1664, 1625	622 (M–Cl)
2g	27.3	7.91–6.83	4.68	5.36, 5.20 (6.4)	2.47, 1.92, 0.83 (6.8)	3324	1683, 1578	614 (M–2Cl)
2h	16.1[b]	7.88–7.46[b]	4.65	5.32, 5.25 (5.8)	2.55, 1.92, 0.93 (6.8)	3321		487 (M–Cl)

[a] Recorded in $CDCl_3/(CD_3)_2SO$.
[b] Recorded in $CDCl_3$.
[c] ^2J(PH) coupling in brackets.
[d] Doublet, ^3J(HH) coupling in brackets.
[e] CH_3, CH and $(CH_3)_2$ protons, respectively, ^3J(HH) coupling in brackets.
[f] About 20% bis-substituted phosphine [δ(P) −27.9 ppm] observed by $^{31}P\{^1H\}$NMR.
[g] About 20% bis-substituted phosphine ruthenium complex [δ(P) 23.4 ppm] observed by $^{31}P\{^1H\}$NMR.

DMSO molecule was modelled with two alternative positions for the S atom [major refined occupancy = 93.9(4)%]. The two MeOH molecules were modelled with C atoms disordered over two positions [major refined occupancies = 52.7(18) and 83.6(17)%], however, no H atoms could be located. In **2h**, the complex containing Ru(2) was modelled with two alternative positions for the Ru, Cl and P atoms and the *p*-cymene ligand [major refined occupancy = 76.3(3)%]. In compounds **2g · 3MeOH**, **2g · DMSO · 1.5MeOH** and **2h**, restraints were applied to the geometry of the disordered groups and the anisotropic displacement parameters of some atoms. Programs used were Bruker AXS SMART and SAINT for diffractometer control and frame integration [38], Bruker SHELXTL for structure solution and refinement [39], Diamond for molecular graphics [40], and local programs. In the following figures, anisotropic displacement ellipsoids are drawn at the 50% probability level. Hydrogen bonds are shown as thin, dashed black lines; the η^6-coordination mode of the *p*-cymene ligand is shown using a thick, dashed grey line between the ruthenium ion and the centroid of the aromatic ring.

Powder X-ray diffraction data were recorded on a Bruker D8 powder diffractometer using monochromated copper radiation over the 2θ range 5–60° using a 0.0147° 2θ step. Simulated powder data were generated from the cif files of the single crystal structures using the program ATOMS v5.0.1 for comparison with the experimental patterns.

3. Results and discussion

3.1. Synthesis and characterisation

We have previously found that Mannich based condensation reactions are extremely facile for the syntheses of functionalised tertiary and ditertiary phosphines [29–34]. Carboxylic acid phosphines [32,34] can be prepared by this procedure and furthermore, we have shown some of these ligands serve as convenient building blocks for the preparation of linear, dinuclear gold(I) complexes [35] with unusual finite and infinite structures. In order to further understand the supramolecular capability of these ligands we turned our attention to half-sandwich organometallic compounds based on ruthenium(II).

Reaction of $NH_2C_6H_4(3\text{-}CO_2H)$ and Ph_2PCH_2OH in a 1:1 molar ratio, in MeOH at ambient temperature, gave $Ph_2PCH_2NHC_6H_4(3\text{-}CO_2H)$ (**1b**) in addition to small amounts (ca. 20%) of the disubstituted phosphine $(Ph_2PCH_2)_2NC_6H_4(3\text{-}CO_2H)$ (Eq. (1)). Both phosphines could readily be distinguished by their characteristic ^{31}P NMR resonances (Table 2) which differ by ca. 10 ppm between both phosphorus species. No attempts were made to purify **1b** which was used directly in the complexation studies.

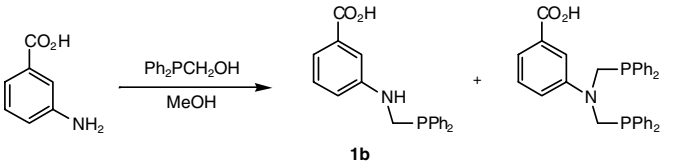

(1)

The ruthenium(II) complexes $RuCl_2(p\text{-cymene})Ph_2PCH_2Y$ [Y = -$NHC_6H_4(2\text{-}CO_2H)$ (**2a**), -$NHC_6H_4(3\text{-}CO_2H)$ (**2b**), -$NHC_6H_3(3\text{-}CO_2H)(6\text{-}OCH_3)$ (**2c**), -$NHC_6H_4(4\text{-}CO_2H)$ (**2d**), -$NHC_6H_3(2\text{-}CO_2H)(4\text{-}OH)$ (**2e**), -$NHC_6H_3(3\text{-}OH)(4\text{-}CO_2H)$ (**2f**), -$NHC_6H_3(2\text{-}CO_2H)(5\text{-}CO_2H)$ (**2g**) and -OH (**2h**)] were prepared by standard bridge cleavage of $\{RuCl_2(p\text{-cymene})\}_2$ [37] with two equivalents of **1a**–**1h** in dichloromethane at room temperature. The $^{31}P\{^1H\}$ NMR data are in good agreement with P-monodentate coordination as inferred by the downfield shift (typically ca. 20 ppm) of their ^{31}P resonances (Table 2). Further supporting evidence is seen in the ^1H NMR spectra showing well resolved signals for the *p*-cymene and PCH_2– [δ(H) 4.34–4.72 ppm] groups. Other characterising data are given in Section 2 and Table 2.

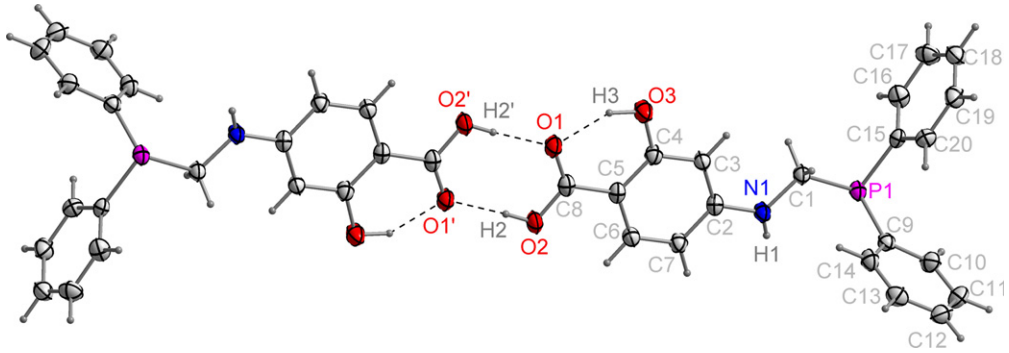

Fig. 1. View of a hydrogen bonded dimer of **1f**. Selected bond lengths and angles for **1f**: P(1)–C(1) 1.8515(18), P(1)–C(9) 1.8254(19), P(1)–C(15) 1.8324(18), C(1)–N(1) 1.454(2), C(8)–O(1) 1.249, C(8)–O(2) 1.320(2) Å. C(1)–P(1)–C(9) 103.73(9), C(1)–P(1)–C(15) 97.70(8), C(9)–P(1)–C(15) 100.70(8), P(1)–C(1)–N(1) 112.45(12)°. Symmetry codes: ′ $-x-1, -y, -z-1$.

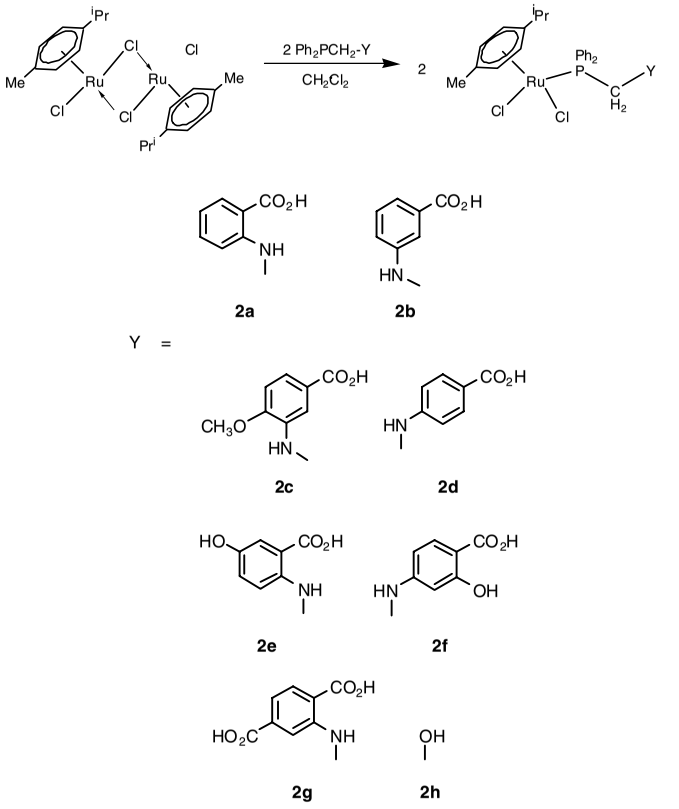

(2)

3.2. Single crystal X-ray diffraction studies

3.2.1. Ligand **1f**

The X-ray structure of the previously reported phosphine **1f** has been determined (Fig. 1) and confirms single condensation has resulted. The geometry about P(1) is pyramidal as expected and bond lengths/angles are similar to those in other crystallographically characterised carboxylic acid modified phosphines [32,34,35,41]. Molecules of **1f** are arranged into head-to-tail dimer pairs [$R_2^2(8)$ graph set motif] [42] via strong O–H···O hydrogen bonding [O(2)···O(1′) 2.6540(19) Å, H···O 1.79(3) Å; O–H···O 177(3)°; symmetry codes: ′ $-x-1$, $-y$, $-z-1$] and the phenol group is involved in intramolecular O–H···O hydrogen bonding with the carbonyl oxygen atom of the carboxylic acid group [O(3)···O(1) 2.5915(19) Å, H···O 1.74(3) Å; O–H···O 146(2)°].

3.2.2. Ruthenium(II) complexes **2a**, **2b** and **2d–2h**

The X-ray structures of **2a**, **2b** and **2d–2h** (Table 3) have been determined and in each case display a classic piano-stool geometry with Ru–P, Ru–Cl or Ru–C_{arene} bond lengths comparable to $RuCl_2$(*p*-cymene)PTA (PTA = 1,3,5-triaza-7-phosphatricyclo[3.3.1.1]-decane) [3], $RuCl_2$-(*p*-cymene)$Ph_2P(2\text{-}C_5H_4N)$ [4] and $RuCl_2$(*p*-cymene)-Ph_2PCH_2Y [Y= -NHC_6H_4(2-OH), -NHC_6H_4(2-CH_2OH)] [31] previously reported.

To investigate how the predisposition and number of functional groups bound to the -N(H)-phenyl scaffold

Table 3
Selected bond distances (Å) and bond angles (°) for compounds **2a**, **2b** · OEt_2 · H_2O, **2d–2f**, **2g** · **3MeOH**, **2g** · **DMSO** · **1.5MeOH** and **2h**

	2a	**2b** · OEt_2 · H_2O	**2d**	**2e**	**2f**	**2g** · **3MeOH**	**2g** · **DMSO** · **1.5MeOH**	**2h**[a]
Bond length (Å)								
Ru(1)–P(1)	2.3292(5)	2.3443(7)	2.3616(10) [2.3423(10)]	2.3347(6)	2.3439(6)	2.3515(13)	2.3486(18) [2.3346(17)]	2.3516(8)
Ru(1)–Cl(1)	2.4166(5)	2.4222(7)	2.4166(9) [2.4357(10)]	2.4202(6)	2.4278(5)	2.4125(12)	2.4167(16) [2.4246(16)]	2.4279(8)
Ru(1)–Cl(2)	2.4233(5)	2.4249(7)	2.4079(9) [2.4176(10)]	2.4362(6)	2.4169(5)	2.4319(12)	2.4060(17) [2.4338(18)]	2.4171(8)
Ru(1)–C_{arene}[b]	1.695	1.701	1.693 [1.699]	1.706	1.705	1.699	1.694 [1.696]	1.710
P(1)–C(11)	1.8590(19)	1.880(3)	1.851(4) [1.848(3)]	1.859(2)	1.878(2)	1.859(5)	1.859(7) [1.860(7)]	1.856(3)
C(11)–N(1)	1.444(2)	1.440(3)	1.452(5) [1.450(5)]	1.442(3)	1.432(3)	1.450(6)	1.441(8) [1.436(8)]	
C–O(1)	1.322(2)	1.312(3)	1.305(5) [1.310(5)]	1.320(3)	1.334(3)	1.319(7)	1.320(8) [1.318(8)]	1.414(5)
C–O(2)	1.241(2)	1.235(4)	1.243(5) [1.250(5)]	1.239(3)	1.230(3)	1.223(7)	1.214(8) [1.228(8)]	
C–O(3)						1.324(6)	1.299(9) [1.326(10)]	
C–O(4)						1.204(7)	1.224(9) [1.196(10)]	
Bond angle (°)								
Cl(1)–Ru(1)–P(1)	85.450(18)	86.12(2)	87.24(3) [87.03(3)]	85.77(2)	87.133(19)	87.58(5)	87.43(6) [86.99(6)]	85.22(3)
Cl(2)–Ru(1)–P(1)	84.386(18)	82.94(2)	84.66(3) [84.36(3)]	85.11(2)	82.823(19)	85.04(5)	84.71(6) [84.25(6)]	87.72(3)
Cl(1)–Ru(1)–Cl(2)	88.725(18)	88.47(2)	88.93(3) [88.26(3)]	86.76(2)	86.816(19)	86.01(4)	85.89(6) [87.52(6)]	87.03(3)
Ru(1)–P(1)–C(11)	112.41(6)	113.17(8)	112.74(12) [111.55(12)]	114.67(7)	113.60(7)	114.84(16)	115.3(2) [114.2(2)]	115.30(12)
P(1)–C(11)–N(1)	114.49(13)	116.70(18)	117.4(3) [116.8(2)]	112.62(15)	117.82(16)	113.7(3)	114.3(4) [114.0(4)]	
P(1)–C(1)–O(1)								112.8(3)

[a] Data given here for the non-disordered molecule only.
[b] Ru···arene distance is taken between the ruthenium(II) ion and the least-squares plane of the aromatic ring of the η^6-*p*-cymene ligand.

influences secondary hydrogen bonding interactions we initially focussed on varying the site of the carboxylic acid group (2-, 3- or 4-position) with respect to the diphenylphosphino moiety. Hence in **2a** (Fig. 2), we find that molecules are linked into head-to-tail dimer pairs [$R_2^2(8)$ graph set motif] through intermolecular O–H···O hydrogen bonding [O(1)···O(2′) 2.641(2) Å, H···O 1.80 Å; O–H···O 176.4°; symmetry codes: ′ $-x$, $1-y$, $1-z$]. Furthermore, the close proximity of the secondary amine group enables additional intramolecular N–H···O hydrogen bonding with the carbonyl oxygen atom of the carboxylic acid group [N(1)···O(2) 2.645(2) Å, H···O 1.98(2) Å; N–H···O 140(2)°] [43].

The 3-substituted isomer **2b** has been structurally characterised as **2b** · $\mathbf{Et_2O}$ · $\mathbf{H_2O}$ upon crystallisation from a CH_2Cl_2/Et_2O solution (Fig. 3). As observed with **2a**, **2b** displays a similar dimer pair association through intermolecular O–H···O hydrogen bonding [O(1)···O(2′) 2.624(3) Å, H···O 1.79 Å; O–H···O 175.3°; symmetry codes: ′ $2-x$, $1-y$, $1-z$]. However, this time due to the remote proximity of the NH group with respect to the carboxylic acid group, no intramolecular N–H··· O hydrogen bonding is observed [43]. Instead the NH group is involved in hydrogen bonding to a water solvate [N(1)···O(4) 2.999(3) Å, H···O 2.16(3) Å; N–H···O 176(3)°]. Hydrogen bonding is also observed between the water and Et_2O solvent molecules [O(4)···O(3) 2.757(4) Å, H···O 1.71(5) Å; O–H···O 165(4)°].

Even when the carboxylic acid group is located at the 4-position a similar motif is found for **2d** (Fig. 4) where again the strong propensity for head-to-tail dimer pair formation is observed for each unique molecule [O(1)···O(2′) 2.643(4) Å, H···O 1.81 Å; O–H···O 173.1° for molecule 1; O(3)···O(4″) 2.615(4) Å, H···O 1.78 Å; O–H···O 175.7° for molecule 2; symmetry codes: ′ $-x$, $2-y$, $-z$; ″ x, $1.5-y$, $0.5+z$]. Utilising the NH group these pairs associate into 12-membered rings [graph set $R_2^2(12)$] via intermolecular N–H···Cl hydrogen bonding [N(1)···Cl(3″)

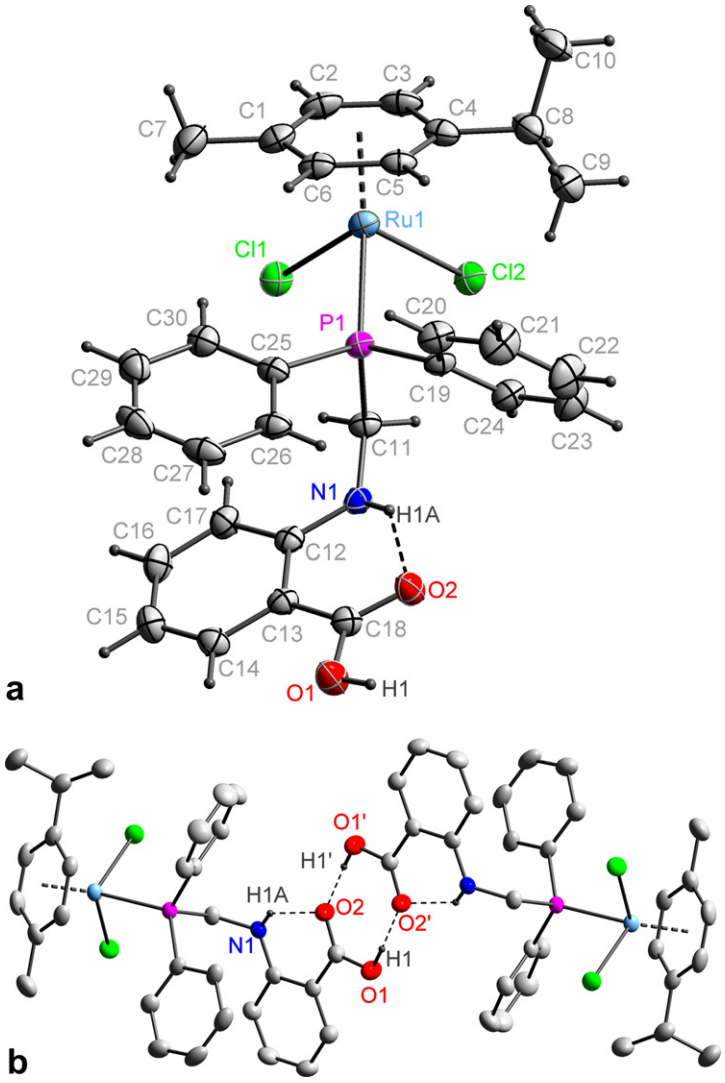

Fig. 2. Views of the (a) molecular and (b) dimeric structures of **2a**. Only the OH and NH hydrogen atoms are shown in (b). Symmetry codes: ′ $-x$, $1-y$, $1-z$.

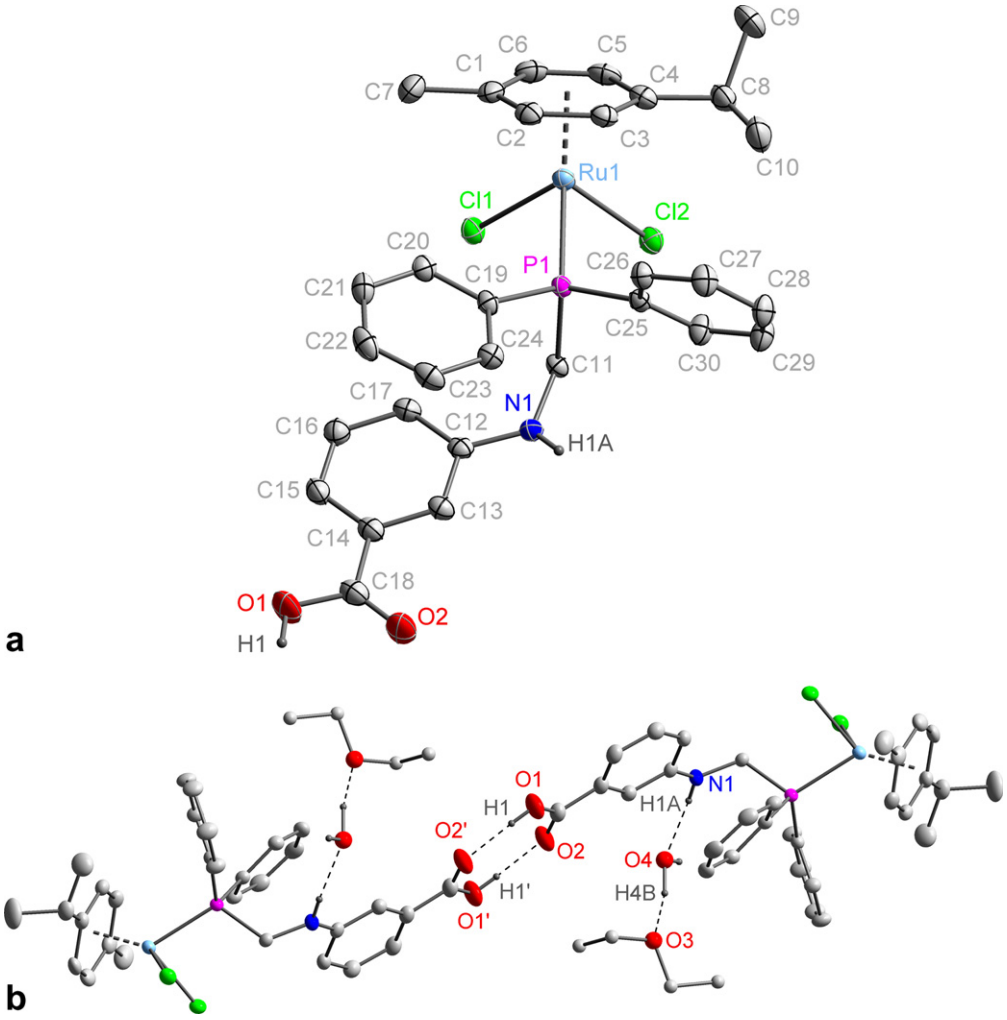

Fig. 3. Views of the (a) molecular and (b) dimeric structure of **2b** · Et_2O · H_2O. Only the OH and NH H-atoms are shown. The H_2O and Et_2O solvent molecules are only shown in (b). Symmetry codes: $'\ 2-x, 1-y, 1-z$.

3.389(3) Å, H···Cl 2.74(4) Å; N–H···Cl 142(4)° for molecule 1; N(2)···Cl(2‴) 3.232(3) Å, H···Cl 2.53(4) Å; N–H···Cl 146(4)° for molecule 2; symmetry codes: $'''x, 1.5-y, z-0.5$] giving rise to 1-D chain motifs.

In summary, the formation of head-to-tail dimer pairs through O–H···O intermolecular H-bonding is observed regardless of the position (2-, 3- or 4-) of the CO_2H group on the tertiary phosphine. These findings reflect the strong desire for hydrogen bonding between neighbouring carboxylic acid groups giving rise to this frequently encountered supramolecular synthon [41,44]. Not surprisingly we also find when the CO_2H group is distanced from the secondary amine, intermolecular N–H···Cl H-bonding (as in **2d**) is preferred over intramolecular N–H···O H-bonding (for **2a**).

Having established the role of the carboxylic acid group predisposition we next sought to consider what effect the introduction of additional polar groups to the -N(H)-phenyl backbone may have on the supramolecular chemistry through alternate hydrogen bonding patterns. In **2e**, retention of the 2-positioned -CO_2H group (with respect to the secondary amine) still gives rise to a head-to-tail motif reminiscent of that seen in **2a** [O(2)···O(1′) 2.647(2) Å, H···O 1.84(3) Å; O–H···O 173(3)°]. The observation of an intramolecular H-bond [N(1)···O(1) 2.677(3) Å, H···O 2.04(3) Å; N–H···O 138(2)°] may play some role in "locking" the -N(H)-arene group into a fixed conformation. In this way the phenolic group gives rise to an overall chain structure that results from intermolecular O–H···Cl hydrogen bonding involving this group and a terminal Ru–Cl ligand [O(3)···Cl(2″) 3.2049(19) Å, H···Cl 2.43(3) Å; O–H···Cl 172(3)°] (Fig. 5). The net effect here is the formation of larger 30-membered hydrogen bonded rings [graph set motif $R_6^4(30)$] in comparison to the 12-membered rings found in **2d**.

In the isomeric complex **2f** in which the -OH and -CO_2H groups are predisposed in 3- and 4-positions, respectively, relative to the –NH group, we see a completely new packing arrangement. The major feature, in stark contrast with **2e** and the uncoordinated ligand **1f**, is the absence of a classic head-to-tail dimer pair. Instead molecules are linked into side-by-side arrangements through intermolecular

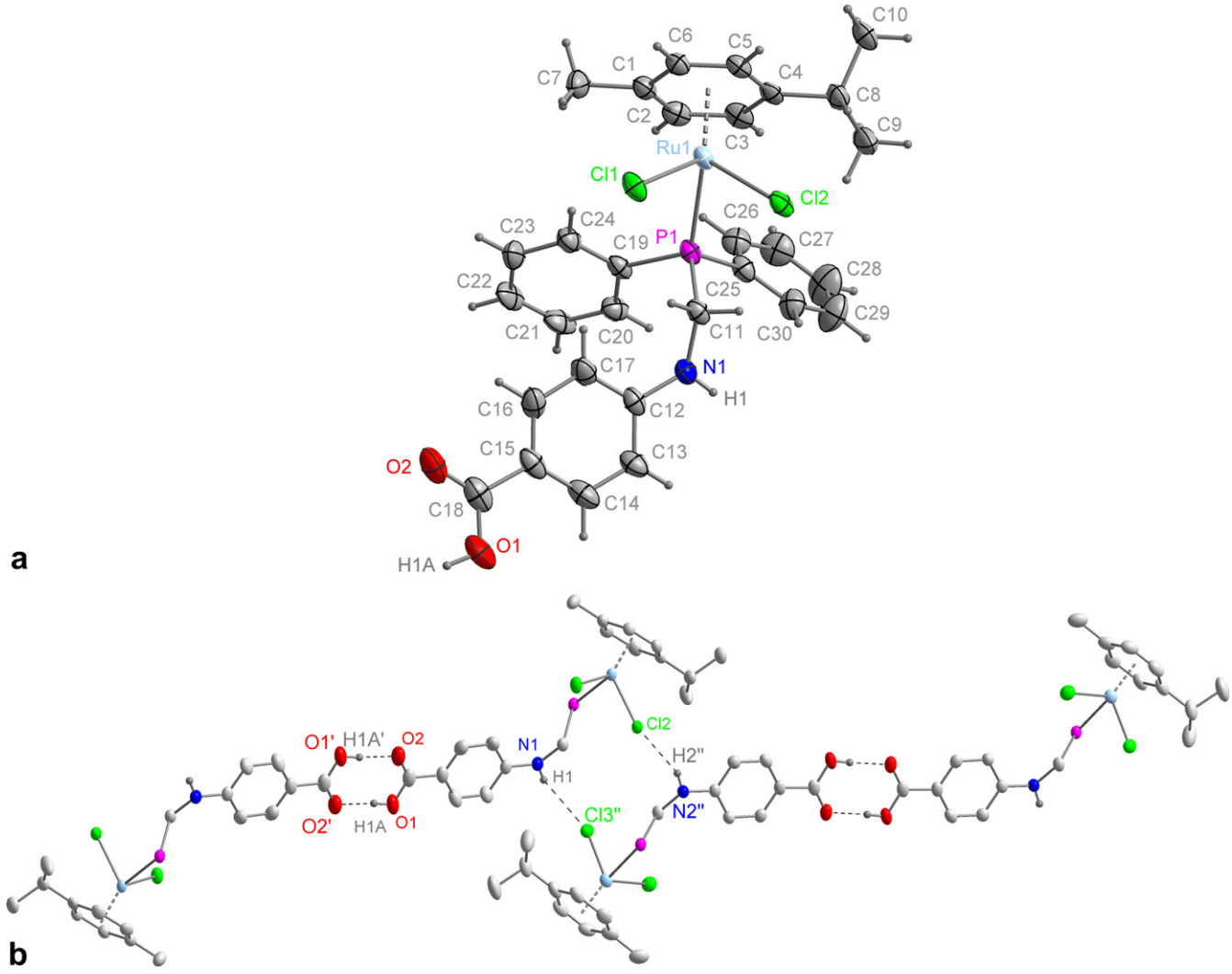

Fig. 4. Views of the (a) molecular structure and (b) extended hydrogen bonded structure of **2d**. Only the OH and NH hydrogen atoms are shown and unsubstituted Ph rings have been removed for clarity in (b). Symmetry codes: $'\ -x, 2-y, -z$; $''\ x, 1.5-y, 0.5+z$.

N–H···O [N(1)···O(3′) 3.251(3) Å, H···O 2.32(3) Å, N–H···O 166(2)°] and O–H···Cl [O(2)···Cl(1″) 3.026(2) Å, H···Cl 2.06(4) Å, O–H···Cl 162(3)°] hydrogen bonding. This leads to alternate 12- and 24-membered rings affording a tape arrangement. The adjacent phenolic OH group is used in forming an intramolecular O–H···O hydrogen bond [O(3)···O(1) 2.615(3) Å, H···O 1.90(3) Å, O–H···O 131(3)°] with the carbonyl oxygen atom of the carboxylic acid group (Fig. 6).

We next looked at the function played by polar solvents on H-bonding arrangements. Compound **2g** was crystallised from two related solvent systems, affording the two solvates **2g · 3MeOH** and **2g · DMSO · 1.5MeOH**. The molecular structure of **2g** is shown in Fig. 7a. In both solvates, the NH group is involved in an intramolecular hydrogen bond with the carbonyl group of the adjacent carboxylic acid group [**2g · 3MeOH** N···O 2.656(6) Å, H···O 1.95(4) Å, N–H···O 135(4)°; **2g · DMSO · 1.5MeOH** N···O 2.647(7)/2.630(7) Å, H···O 1.94/1.92 Å, N–H···O 136/137°]. This feature resembles that found with **2a** and **2e**. The solvate **2g · 3MeOH** was crystallised via the vapour diffusion of Et_2O into a $CDCl_3$/MeOH solution of **2g**. There are no direct hydrogen bonds between molecules of **2g** in **2g · 3MeOH**, instead the molecules are linked by MeOH molecules into tapes propagating in the crystallographic [−1 0 1] direction. The MeOH molecules are essentially inserted into (carboxylic acid)O–H···Cl hydrogen bonds, leading to two hydrogen bonding motifs. In the first motif, one MeOH molecule has been inserted giving a CO_2H···MeOH···Cl sequence [O(2)···O(5) 2.663(6) Å, H···O 1.83 Å, O–H···O 172°; O(5)···Cl(2′) 3.133(4) Å, H···Cl 2.30 Å, O–H···Cl 169°, symmetry codes: $'\ x+0.5, 0.5-y, z-0.5$]. In the second motif, two MeOH molecules have been inserted giving a CO_2H···MeOH···MeOH···Cl sequence [O(4)···O(6) 2.616(8) Å, H···O 1.78 Å, O–H···O 178°; O(6)···O(7) 2.666(9) Å, H···O 1.91 Å, O–H···O 149°; O(7)···Cl(1″) 3.138(5), H···Cl 2.31 Å, O–H···Cl 167°, symmetry codes: $''\ x-0.5, 0.5-y, z+0.5$] (Fig. 7b).

The solvate **2g · DMSO · 1.5MeOH** was crystallised from the vapour diffusion of Et_2O into a $CDCl_3$/MeOH/

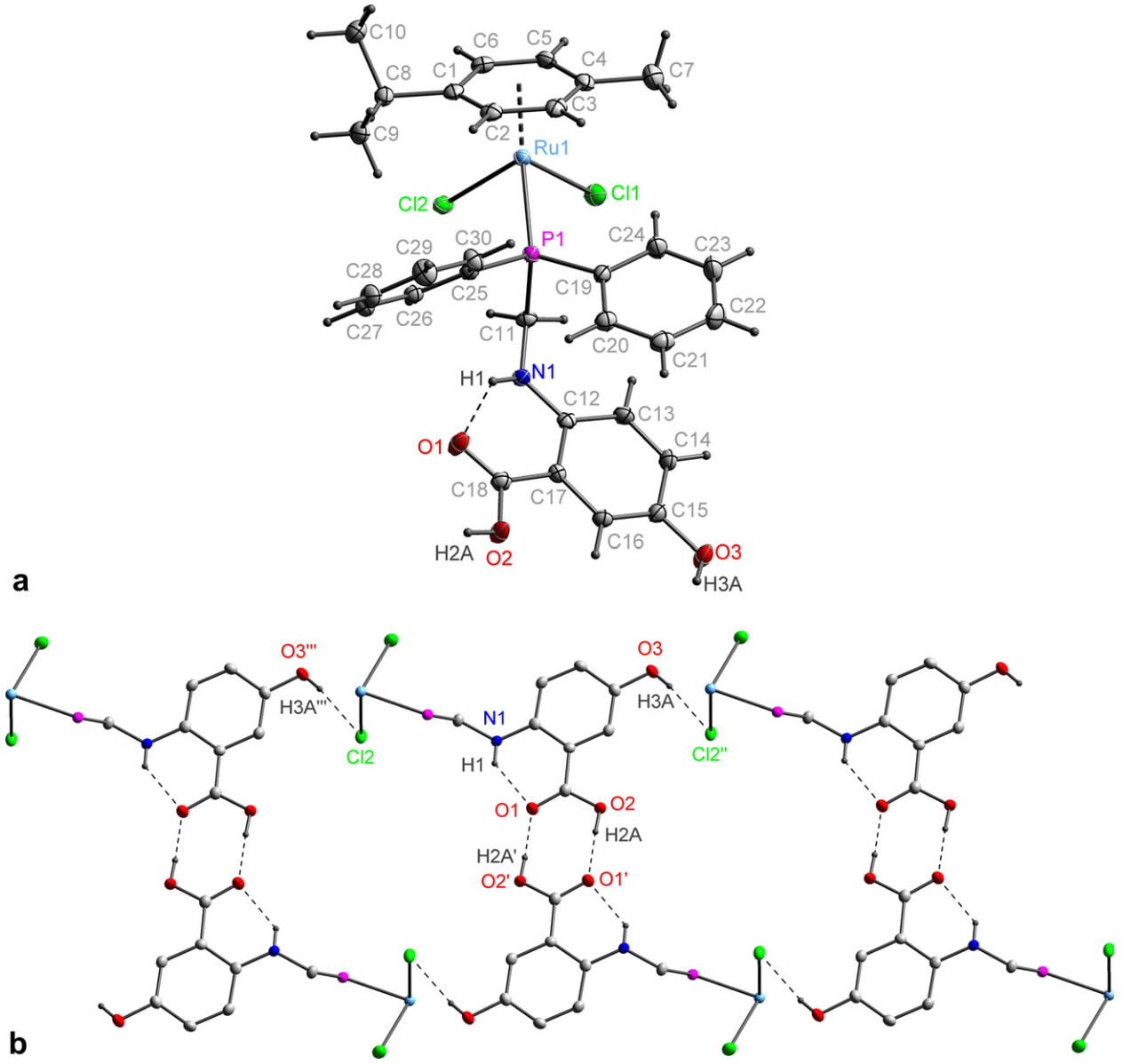

Fig. 5. Views of the (a) molecular structure and (b) extended hydrogen bonded structure of **2e**. Only the O–H and N–H hydrogen atoms are shown and unsubstituted Ph rings and *p*-cymene ligands have been removed for clarity in (b). Symmetry codes: ′ $1-x, 1-y, -z$; ″ $x, y+1, z$; ‴ $x, y-1, z$.

DMSO solution of **2g**. As observed in **2g · 3MeOH**, there are no hydrogen bonds between the two unique half-sandwich complexes in **2g · DMSO · 1.5MeOH**; both unique complexes are involved in different hydrogen bonding patterns. Each complex has one CO_2H group hydrogen bonded to a DMSO molecule through the combination of a strong O–H···O and a weaker C–H···O hydrogen bond using a methyl CH group of the DMSO molecule forming a $R_2^2(7)$ graph set motif [molecule containing Ru(1): O(1)···O(10) 2.589(7) Å, H···O 1.76 Å, O–H···O 170°; C(66)···O(2) 3.191(9) Å, H···O 2.34 Å, C–H···O 144°; molecule containing Ru(2): O(5)···O(9) 2.596(8) Å, H···O 1.80 Å, O–H···O 158°; C(64)···O(6) 3.434(10) Å, H···O 2.58 Å, C–H···O 146°]. The DMSO molecules hydrogen bond to one of the two CO_2H groups in each complex, with the choice of CO_2H group leading to the existence of two hydrogen bonding patterns. In one complex/DMSO adduct, the CO_2H group involved is adjacent to the NH group, while in the second complex/DMSO adduct, the CO_2H group involved is positioned further from the NH group.

The CO_2H groups lacking interactions with DMSO form hydrogen bonds to MeOH molecules, resulting in CO_2H···MeOH···Cl [O(3)···O(13) 2.748(13) Å, H···O 1.91 Å, O–H···O 173°; O(12)···Cl(1) 3.061(8) Å; O(13)···O(12″) 2.654(15) Å, symmetry codes: ″ $x, 1.5-y, z+0.5$] and CO_2H···MeOH···MeOH···Cl motifs [O(7)···O(11) 2.711(9) Å, H···O 1.91 Å, O–H···O 159°; O(11)···Cl(4′) 3.270(6) Å, symmetry codes: ′ $x, 1.5-y, z-0.5$], as observed in **2g · 3MeOH**. Two unique sets of

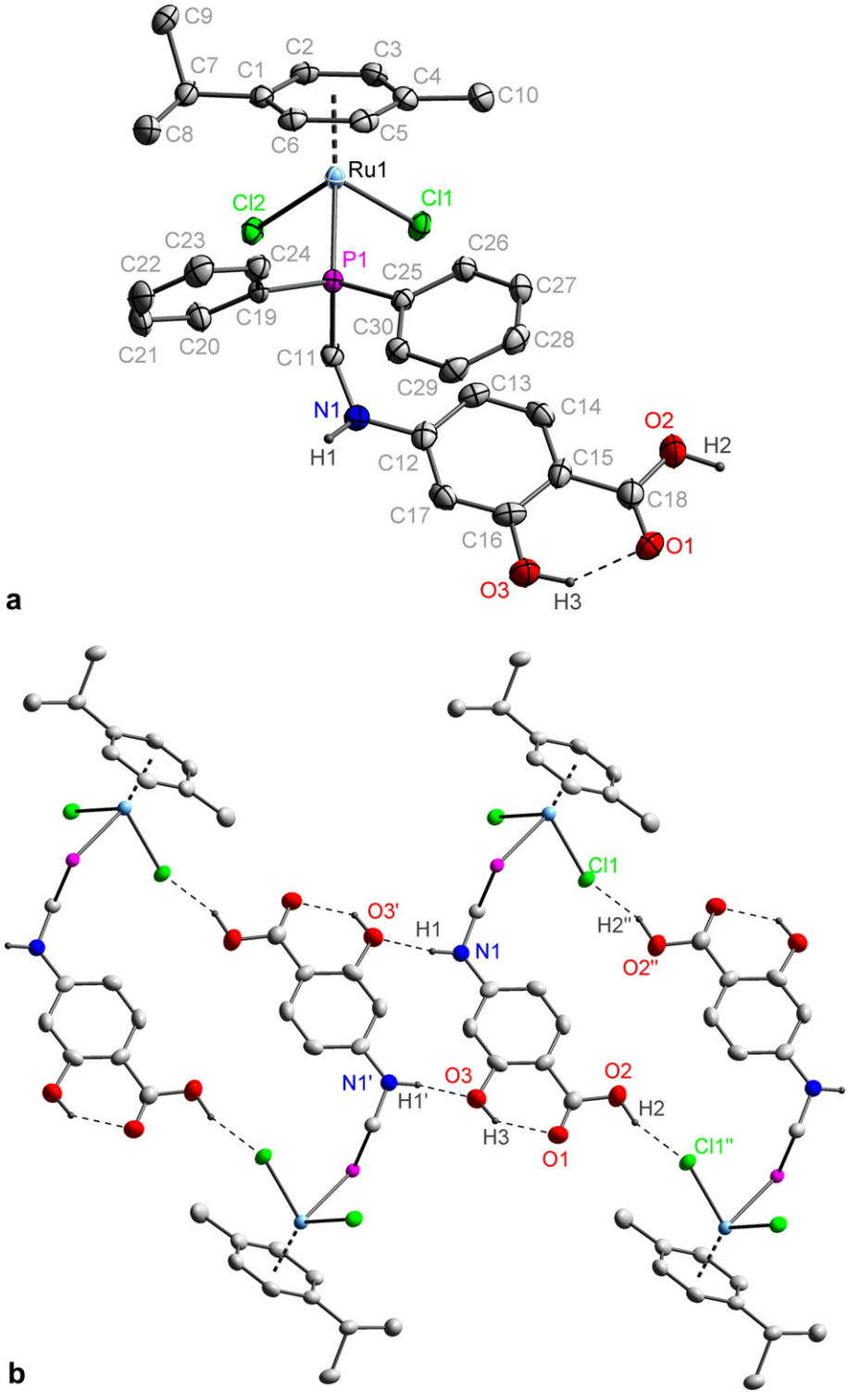

Fig. 6. Views of the (a) molecular structure and (b) extended hydrogen bonded structure of **2f**. Only the O–H and N–H hydrogen atoms are shown; unsubstituted Ph rings have been removed for clarity in (b). Symmetry codes: $'$ $-x-1, 1-y, -z$; $''$ $-x-1, 2-y, -z$.

chains are formed, both propagating parallel to the crystallographic *c* axis. It is clear from a comparison of Fig. 7b and Fig. 8a and b that the DMSO molecules have inserted into the hydrogen bonding motifs observed in **2g** · **3MeOH**, disrupting the tape structure of **2g** · **3MeOH** to create zig-zag chains.

In order to demonstrate the importance of the $-CO_2H$ and –OH groups attached to the -N(H)-arene backbone we also determined the X-ray structure of **2h** (Fig. 9). In each independent molecule there is only one intramolecular O–H···Cl hydrogen bond [O(1)···Cl(1) 3.102(3) Å, H···Cl 2.274(18) Å; O–H···Cl 165(5)° for molecule 1; O(2)···Cl(4)

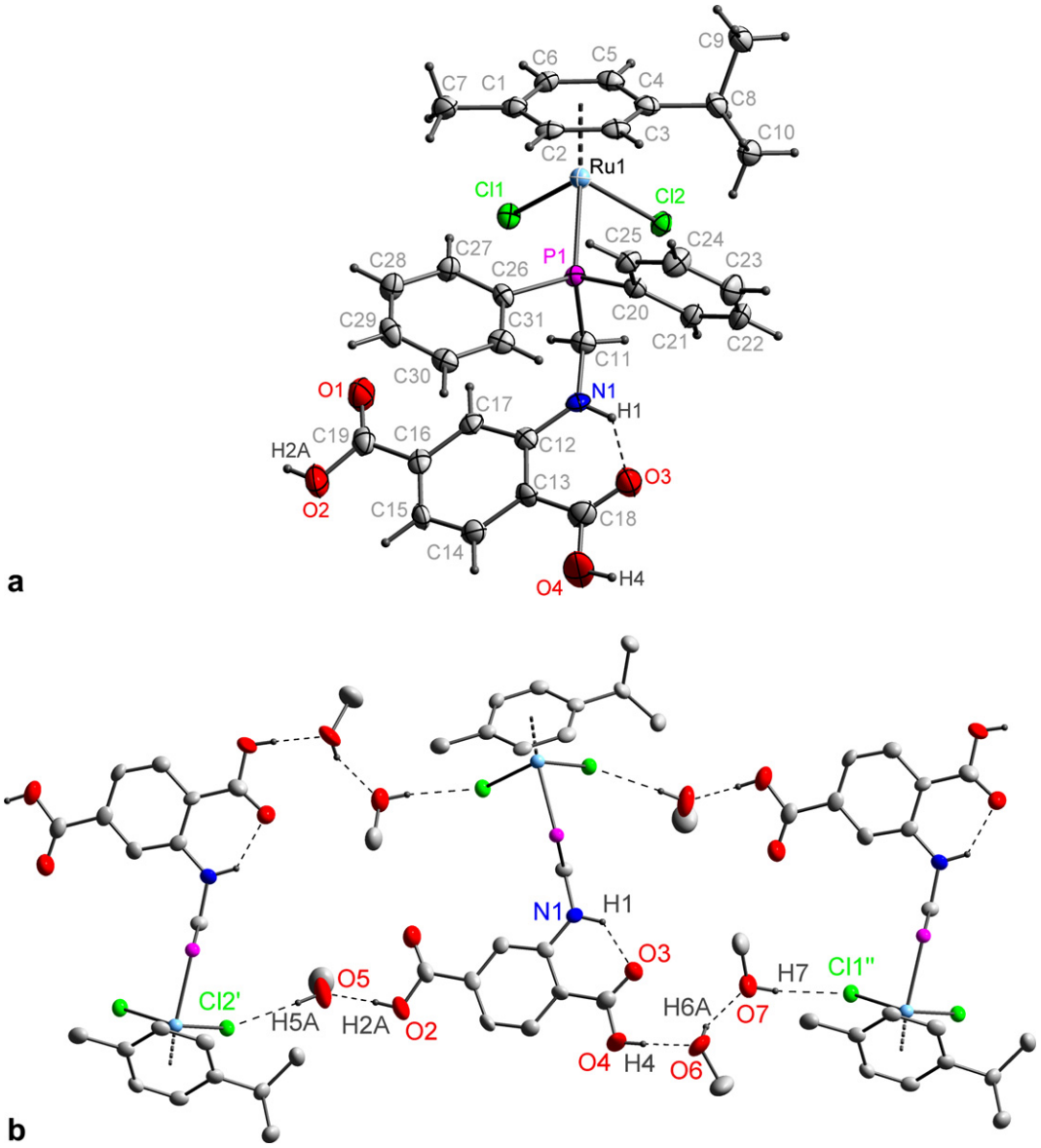

Fig. 7. Views of the (a) molecular structure and (b) extended hydrogen bonded structure of **2g** · **3MeOH**. Only the OH and NH hydrogen atoms are shown and unsubstituted Ph rings have been removed for clarity in (b). The MeOH solvent molecules are not shown in (a). Symmetry codes: $'\ x+0.5, 0.5-y, z-0.5$; $''\ x-0.5, 0.5-y, z+0.5$.

3.151(4) Å, H···Cl 2.35(2) Å; O–H···Cl 160(5)° for molecule 2]. This observation is similar to that previously reported by Therrien and co-workers who noted a similar intramolecular O–H···Cl hydrogen bond in the ruthenium(II) complex $RuCl_2\{\eta^6\text{-}C_6H_5(CH_2)_3OH\}(PPh_3)$ [27b]. Hence while the functionalisation of the tertiary phosphine/arene ligands has, in effect, been reversed the propensity for this type of secondary interaction is evident here.

3.3. Powder X-ray diffraction studies

We have also performed some preliminary powder X-ray diffraction studies with four representative examples namely **2a**, **2d**, **2e** and **2f**. The experimental powder patterns of **2a** and **2f** are in excellent agreement with the simulated powder patterns that were derived from their single crystal X-ray structures. This implies the hydrogen bonding arrangements hypothesised in the single crystal determination are present in the bulk unrecrystallised material and have not been directed by the solvent used for single crystal growth. However, in the powder pattern of **2e**, additional reflections are exhibited that are extraneous to those presented in the theoretical pattern indicating that the bulk unrecrystallised sample is probably a mixture of phases. Finally, the powder diffraction data collected from the bulk **2d** unrecrystallised sample is in poor agreement with the theoretical pattern generated from the single crystal study implying the possible presence of some impurities and/or the solvent

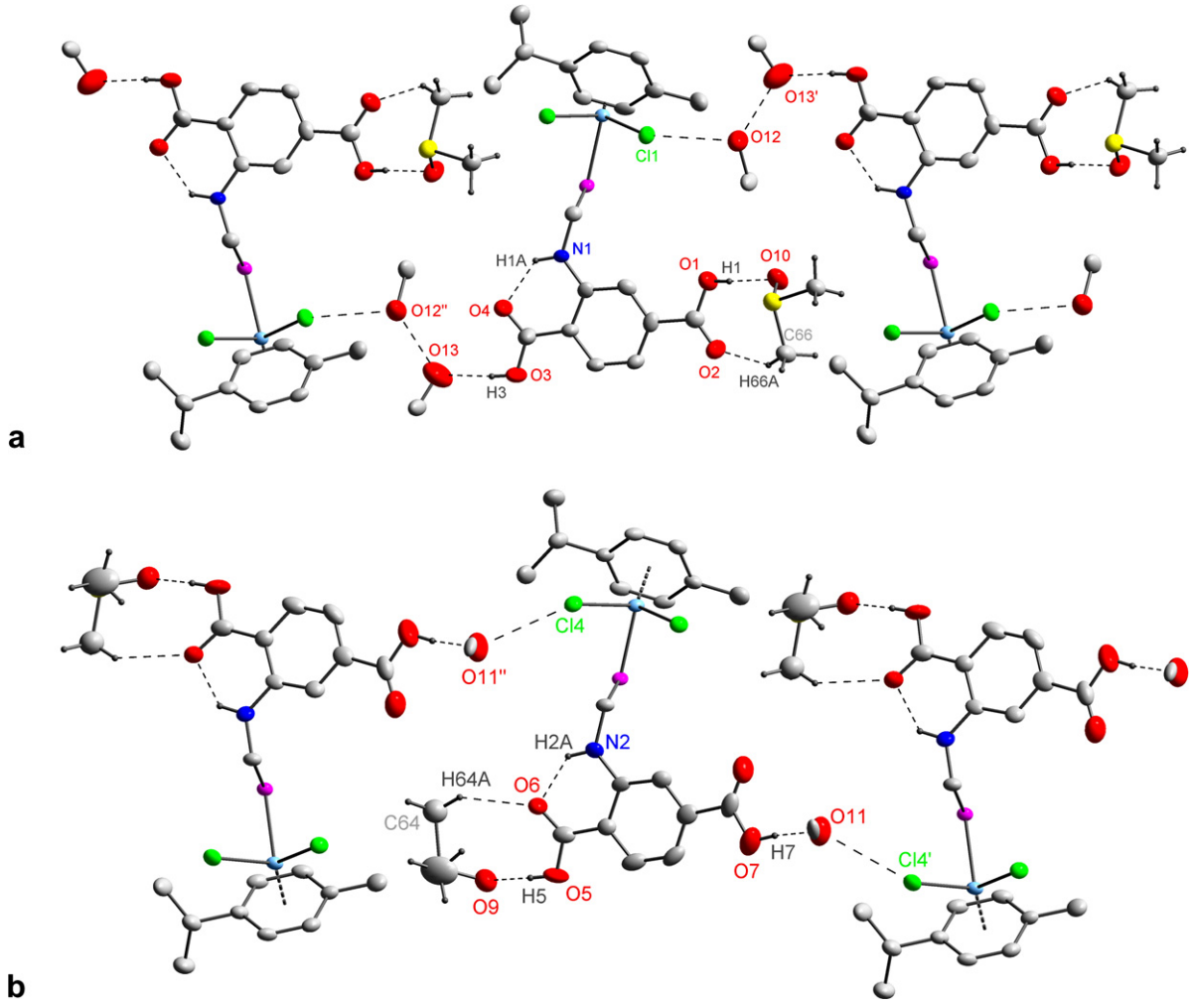

Fig. 8. Views of the extended hydrogen bonded structure of **2g · DMSO · 1.5MeOH**, showing two unique chains formed by (a) molecules containing Ru(1) and (b) molecules containing Ru(2). Only the OH, NH and methyl hydrogen atoms are shown and unsubstituted Ph rings have been removed for clarity. Symmetry codes: $'$ x, $1.5-y$, $z-0.5$; $''$ x, $1.5-y$, $z+0.5$.

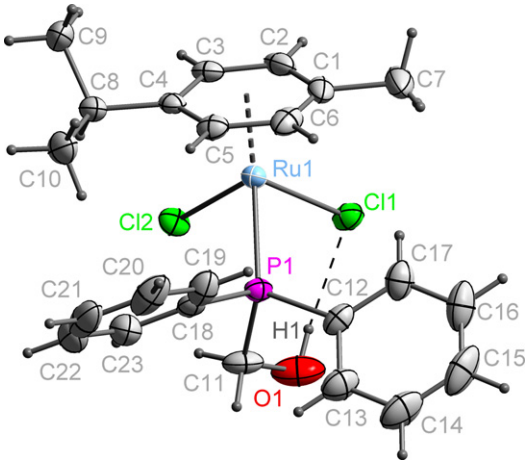

Fig. 9. View of the molecular structure of **2h** showing only one of the two independent molecules.

used for single crystal growth has had a structure directing affect and coordinated to the moieties during crystallisation.

4. Conclusions

Our studies with organometallic half-sandwich ruthenium(II) complexes containing highly functionalised monodentate tertiary phosphines has revealed that a variety of self-assembled structures can be achieved. The predominant manner by which these supramolecular architectures can be controlled utilises the type and position of the functional group(s) on the tertiary phosphine. Furthermore, the choice of highly polar recrystallisation solvents such as MeOH/DMSO disrupts any strong O–H···O H-bonding between carboxylic acid groups in favour of extended structures that incorporate DMSO and/or MeOH molecules. Further systematic studies of these isomeric ligands towards other metal centres are in progress and will be reported in due course.

Acknowledgements

We are grateful to Johnson-Matthey for the kind donation of $RuCl_3 \cdot xH_2O$ and the EPSRC Mass Spectrometry

Service centre at Swansea. We also thank the Leverhulme Trust (S.T.) and EPSRC (S.E.D., P.M.S.) for funding.

Appendix A. Supplementary material

A complete set of X-ray crystallographic structural data for compounds **1f**, **2a**, **2b** · Et_2O · H_2O, **2d**–**2f**, **2g** · **3MeOH**, **2g** · **DMSO** · **1.5MeOH** and **2h** (CCDC Nos. 295350–295358, respectively) is available at the Cambridge Crystallographic Data Centre, 12 Union Road, Cambridge CB2 1EZ, UK (fax: +44 1223 336 033; e-mail: deposit@ccdc.cam.ac.uk) on request, quoting the deposition numbers. Supplementary data associated with this article can be found, in the online version, at doi:10.1016/j.jorganchem.2006.07.036.

References

[1] V. Cadierno, J. Díez, S.E. García-Garrido, S. García-Grando, J. Gimeno, J. Chem. Soc., Dalton Trans. (2002) 1465.
[2] D. Drommi, C. Grazia Arena, F. Nicolò, G. Bruno, F. Faraone, J. Organomet. Chem. 485 (1995) 115.
[3] R. Lalrempuia, P.J. Carroll, M.R. Kollipara, J. Chem. Sci. 116 (2004) 21.
[4] A. Dorcier, P.J. Dyson, C. Gossens, U. Rothlisberger, R. Scopelliti, I. Tavernelli, Organometallics 24 (2005) 2114.
[5] O. Novakova, H. Chen, O. Vrana, A. Rodgers, P.J. Sadler, V. Brabec, Biochemistry 42 (2003) 11544.
[6] H. Chen, J.A. Parkinson, R.E. Morris, P.J. Sadler, J. Am. Chem. Soc. 125 (2003) 173.
[7] (a) A. Buryak, K. Severin, J. Am. Chem. Soc. 127 (2005) 3700;
(b) Z. Grote, R. Scopelliti, K. Severin, J. Am. Chem. Soc. 126 (2004) 16959.
[8] L. Ion, D. Morales, J. Pérez, L. Riera, V. Riera, R.A. Kowenicki, M. McPartlin, Chem. Commun. (2006) 91.
[9] C.A. Mebi, B.J. Frost, Organometallics 24 (2005) 2339.
[10] D. Jan, L. Delaude, F. Simal, A. Demonceau, A.F. Noels, J. Organomet. Chem. 606 (2000) 55.
[11] (a) C. Letondor, A. Pordea, N. Humbert, A. Ivanova, S. Mazurek, M. Novic, T.R. Ward, J. Am. Chem. Soc. 128 (2006) 8320;
(b) M.T. Reetz, X. Li, J. Am. Chem. Soc. 128 (2006) 1044;
(c) I. Schiffers, T. Rantanen, F. Schmidt, W. Bergmans, L. Zani, C. Bolm, J. Org. Chem. 71 (2006) 2320;
(d) A. Ros, A. Magriz, H. Dietrich, R. Fernández, E. Alvarez, J.M. Lassaletta, Org. Lett. 8 (2006) 127;
(e) P. Pelagatti, M. Carcelli, F. Calbiani, C. Cassi, L. Elviri, C. Pelizzi, U. Rizzotti, D. Rogolino, Organometallics 24 (2005) 5836;
(f) V. Cadierno, P. Crochet, J. Díez, J. García-Álvarez, S.E. García-Garrido, J. Gimeno, Inorg. Chem. 42 (2003) 3293.
[12] M. Ito, S. Kitahara, T. Ikariya, J. Am. Chem. Soc. 127 (2005) 6172.
[13] J.-B. Sortais, V. Ritleng, A. Voelklin, A. Holuigue, H. Smail, L. Barloy, C. Sirlin, G.K.M. Verzijl, J.A.F. Boogers, A.H.M. de Vries, J.G. de Vries, M. Pfeffer, Org. Lett. 7 (2005) 1247.
[14] D.L. Davies, O. A-Duaij, J. Fawcett, M. Giardiello, S.T. Hilton, D.R. Russell, Dalton Trans. (2003) 4132.
[15] K.G. Gaw, A.M.Z. Slawin, M.B. Smith, Organometallics 18 (1999) 3255.
[16] P. Pinto, G. Marconi, F.W. Heinemann, U. Zenneck, Organometallics 23 (2004) 374.
[17] C. Ganter, Chem. Soc. Rev. 32 (2003) 130.
[18] K.K. Klausmeyer, T.B. Rauchfuss, S.R. Wilson, Angew. Chem., Int. Ed. Engl. 37 (1998) 1694.
[19] Y. Yamamoto, H. Suzuki, N. Tajima, K. Tatsumi, Chem. Eur. J. 8 (2002) 372.
[20] C. Lidrissi, A. Romerosa, M. Saoud, M. Serrano-Ruiz, L. Gonsalvi, M. Peruzzini, Angew. Chem., Int. Ed. 44 (2005) 2568.
[21] L. Brammer, Chem. Soc. Rev. 33 (2004) 476.
[22] (a) L. Brammer, J.C. Mareque Rivas, R. Atencio, S. Fang, F.C. Pigge, J. Chem. Soc., Dalton Trans. (2000) 3855;
(b) R. Atencio, L. Brammer, S. Fang, F.C. Pigge, New J. Chem. 23 (1999) 461.
[23] M. Oh, G.B. Carpenter, D.A. Sweigart, Acc. Chem. Res. 37 (2004) 1.
[24] D. Braga, L. Maini, M. Polito, L. Scaccianoce, G. Cojazzi, F. Grepioni, Coord. Chem. Rev. 216–217 (2001) 225.
[25] S.U. Son, J.A. Reingold, G.B. Carpenter, D.A. Sweigart, Chem. Commun. (2006) 708.
[26] (a) A. Schlüter, K. Bieber, W.S. Sheldrick, Inorg. Chim. Acta 340 (2002) 35;
(b) D. Vichard, M. Gruselle, H. El Amouri, G. Jaouen, J. Vaissermann, Organometallics 11 (1992) 976.
[27] (a) C. Scolaro, T.J. Geldbach, S. Rochat, A. Dorcier, C. Gossens, A. Bergamo, M. Cocchietto, I. Tavernelli, G. Sava, U. Rothlisberger, P.J. Dyson, Organometallics 25 (2006) 756;
(b) B. Therrien, L. Vieille-Petit, J. Jeanneret-Gris, P. Štěpnička, G. Süss-Fink, J. Organomet. Chem. 689 (2004) 2456;
(c) J. Soleimannejad, C. White, Organometallics 24 (2005) 2538;
(d) J. Soleimannejad, A. Sisson, C. White, Inorg. Chim. Acta 352 (2003) 121;
(e) J.L. Snelgrove, J.C. Conrad, G.P.A. Yap, D.E. Fogg, Inorg. Chim. Acta 345 (2003) 268.
[28] S.A. Serron, S.P. Nolan, Organometallics 14 (1995) 4611.
[29] S.E. Durran, M.B. Smith, A.M.Z. Slawin, J.W. Steed, J. Chem. Soc., Dalton Trans. (2000) 2771.
[30] S.J. Coles, S.E. Durran, M.B. Hursthouse, A.M.Z. Slawin, M.B. Smith, New J. Chem. 25 (2001) 416.
[31] S.E. Durran, M.B. Smith, A.M.Z. Slawin, T. Gelbrich, M.B. Hursthouse, M.E. Light, Can. J. Chem. 79 (2001) 780.
[32] M.B. Smith, M.R.J. Elsegood, Tetrahedron Lett. 43 (2002) 1299.
[33] S.E. Durran, M.B. Smith, M.R.J. Elsegood, New J. Chem. 26 (2002) 1402.
[34] S.E. Durran, M.R.J. Elsegood, N. Hawkins, M.B. Smith, S. Talib, Tetrahedron Lett. 44 (2003) 5255.
[35] M.B. Smith, S.H. Dale, S.J. Coles, T. Gelbrich, M.J. Hursthouse, M.E. Light, CrystEngComm 8 (2006) 140.
[36] H. Hellmann, J. Bader, H. Birkner, O. Schumacher, Liebigs Ann. Chem. 659 (1962) 49.
[37] M.A. Bennett, A.K. Smith, J. Chem. Soc., Dalton Trans. (1974) 233.
[38] SMART and SAINT software for CCD diffractometers, Bruker AXS Inc., Madison, WI, 2001.
[39] G.M. Sheldrick, SHELXTL: User Manual, Version 5.1, Bruker ACS Inc., Madison, WI, 1999.
[40] K. Brandenburg, Diamond Version 3.0e, Crystal Impact GbR, Bonn, Germany, 2005.
[41] P. Štěpnička, Eur. J. Inorg. Chem. (2005) 3787.
[42] M.C. Etter, J.C. MacDonald, J. Bernstein, Acta Crystallogr., Sect. B 46 (1990) 256;
J. Bernstein, R.E. Davis, L. Shimoni, N.-L. Chang, Angew. Chem., Int. Ed. Engl. 34 (1995) 1555.
[43] X. Mei, A.T. August, C. Wolf, J. Org. Chem. 71 (2006) 142.
[44] M.-C. Tse, K.-K. Cheung, M.C.-W. Chan, C.-M. Che, Chem. Commun. (1998) 2295.